Microfluidic T-Form Mixer Utilizing Pressure Disturbances

YB Ma[*], M. Fields[*], CP Sun[*], FY Zhang[**], JC. Liao[***], Y.Li[***], B.M. Churchill[***] and CM Ho[*]

[*] Department of Mechanical and Aerospace Engineering, UCLA
Room 48-121, 420 Westwood, Los Angeles, CA 90095, yanbao@seas.ucla.edu
[**]M 330, Spencer Lab,Department of Mechanical Engineering
University of Delaware, Newark, DE 19711 fyzhang@udel.edu
[***] Urology Department, UCLA, Los Angeles, USA, JCLiao@mednet.ucla.edu

ABSTRACT

A simple solution to mixing problems in micro fluidic systems was presented in this paper. A T-form microfluidic mixer was designed and tested utilizing pressure disturbances. The performance of the mixer was studied through both numerical simulation and experimentation. Based on results of numerical simulation, more than 75% mixing can be finished within a mixing distance of less than 1.5mm from the T-junction for flow with Reynolds number less than 0.24. For Reynolds number higher than 0.24, about 90% mixing can be finished in less than 1.5mm. The numerical results were validated by mixing two aqueous solutions under the microscope and the flow field was visualized using two different dyes. There was very good agreement between the numerical simulation results and experimental results in flow patterns.

Keywords: T-mixer, micro fluidic, pressure disturbances, numerical simulation, experimentation

1 INTRODUCTION

Recently, micro total analysis systems (μTAS) and lab-on-a-chip have attracted enormous attentions due to rapid development in micro fabrication technology and their promising application in biology and biotechnology including fundamental biological research, biomedical diagnostics and therapeutics [1][2]. Micro fluidic mixing is required for most μTAS as it can significantly reduce the overall processing time of the system. In micro-fluidic systems, the flow is typically laminar due to small geometry and viscous dissipation. As a result, mixing in micro reactors stands out as one of the most time-consuming fluidic processes, even after all the advances made in lab-on-a-chip devices.

Two types of micro mixer, passive mixer and active mixer have been reported. For passive mixer, there is no moving part or external energy to enhance mixing. The passive mixer is typically based on design of three dimensional complex geometries to split and recombine channels in order to increase the contact interface and decrease required diffusion distance. However, it is a complicated process to fabricate three-dimensional complex channels. For design of active mixers, ultrasonic vibration, magnetohydrodynamic (MHD) convection and magnetic stirring have been successfully used to generate external forces to perform active mixing of fluids in micro channels. The recent progress in the design of micro mixers was reviewed in [4-6]. Chaotic advection is an efficient mechanism that can enhance mixing in a usually diffusion dominated mixing in laminar flow. Especially, chaotic mixing can be generated in simple two-dimensional micro channels [5]. T-form mixer was studied by Aubry's group [7-8]. However, flow phenomena in micro channel at different Reynolds number needs further analysis. In this paper, the performance of T-form mixer was investigated by using CFD-ACE+ for numerical analysis and experiment for visualization of the flow field and validation of the design. Efficient mixing was achieved within a mixing distance of less than 1.5mm from the T-junction for flow rates ranging from 0.2μl/min to 10μl/min. In addition, we found there were big differences in mixing degree at different flow Reynolds number, which can be explained by different flow phenomena at different Reynolds number.

2 COMPUTATIONAL SIMULATION

2.1 Numerical methods

Computational fluid dynamics (CFD) simulations were applied to guide the design of the T-form micro mixer using CFD-ACE+ (ESI North America, Bloomfield Hills, USA). The coordinates and dimensions of the T-mixer model are shown in Fig. 1. The main mixing channel (horizontal) is 3mm long and 196μm wide, while the vertical channel before confluence is 1.2mm long and 117μm wide. In our original design, the width of main channel is 200μm and that of vertical channel is 100 μm. After fabrication of the mixer by using photolithography, the real width of the channels was measured as 196 μm and 117 μm, respectively. The difference in channel width between the designed value and real value is due to defect in fabrication. Therefore, we use the real width of channels in our simulations. Two dimensional simulations are used with structured grids. For the vertical channel before confluence, 21 grids points are used in x direction

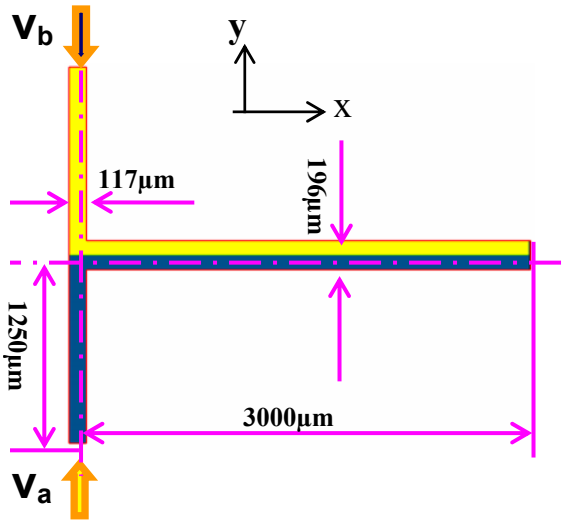

Figure 1. Dimensions and coordinates of the T-form mixer model.

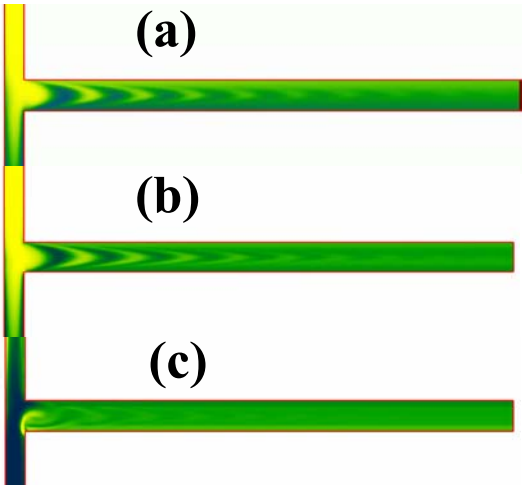

Figure 2. Contours of species concentration at different flow rates from numerical simulation: (a) Re = 0.048, F = 2 Hz. (b) Re = 0.24, F = 10 Hz. (c) Re = 2.4, F = 100 Hz.

and 83 points in y direction. For main mixing channel, 151 points are used in x direction and 41 points in y direction. We have conducted numerical experiment by doubling the grids and found that the numerical error is less than 2%. This means the numerical results are grids independent. Two aqueous solutions with different concentrations represented by different color (blue and yellow) are introduced through inlets A and B. For inlet A, the concentration is 0.0M and it is 0.01M for inlet B. The inflow velocities are specified as V_a and V_b, respectively. $V_{a,b} = V_0 + V_d \sin(2.0\pi ft + \varphi_{a,b})$, where V_0 stands for mean flow velocity, V_d is velocity disturbance from pressure perturbation, f is disturbance frequency, and phase angle $\varphi_a = 0$, $\varphi_b = 180^o$. For all different design of micro mixer, the typical method to enhance mixing is to increase interface area between two different solutions, but the final process of mixing is still through molecular diffusion. In the numerical simulation, the diffusion coefficient is set to be $D = 10^{-10}$ m^2s^{-1}, which is typical value for most biomolecules, such as RNA, DNA and proteins. The kinetic viscosity, υ, is set to be 10^{-6} m^2s^{-1} equal to that of water. The time step for unsteady simulations is set to 50 steps per cycle of periodical disturbances. A characteristic length scale L is defined as:

$$L = 2\frac{A}{W + H} \qquad (1)$$

where A = W*H, is wetted area, W is the width of the main channel (W = 196 µm), and H is the height of the channel (H = 82 µm measured after fabrication). From eqn. (1), L is calculated as 115.6 µm. For mean base flow rate Q = 1.0 µl / min, flow Reynolds number is 0.12 calculated from

$$\mathrm{Re} = VL/\nu \qquad (2)$$

where V is the mean velocity at the exit of the main mixing channel (V = 1.035mm/s for Q = 1.0µl / min). For periodical flow, the Strouhal number is usually used to characterize different time scales, which is defined as the ratio of the characteristic time of the flow to the disturbance period:

$$St = \frac{L/V}{1/f} \qquad (3)$$

2.2 Numerical results

The unsteady flow fields were simulated until the flow reached a periodical state. Figure 2 displays contours of species concentration at fixed St = 0.56 and different flow rates with Re = 0.048, 0.24 and 2.4. The corresponding flow rates are 0.4, 2.0 and 20.0µl/min for (a), (b) and (c) respectively. Two different solutions with two different concentrations, 0.01M and 0.0M represented by yellow and blue respectively, mixed together in the main mixing channel. Without disturbances, there is a distinct interface between yellow and blue solutions as shown in Fig.1. For results shown in Fig.2, the amplitude of disturbances in term of V_d / V_0 is fixed as 20. The disturbance frequency is 2Hz for (a), 10 Hz for (b) and 100 Hz for (c). It is obvious that the flow patterns in (a) for Re = 0.048 are very similar to that in (b) for Re = 0.24. This is because the flow is viscous dominant while the nonlinear effects from inertial terms are negligible at such low Reynolds number. The yellow and blue solutions in (a) and (b) are split into alternate small pieces, which can significantly increase the interface area for molecular diffusion. While the interface is clear near the T-junction, it gradually blurred downstream due to molecular diffusion. As a result, the color of the mixture turns green. For higher Reynolds number flow shown in Fig.2 (c) (Re = 2.4), the

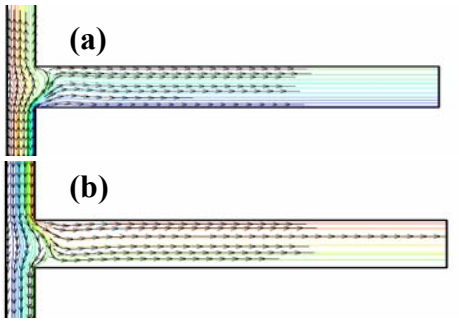

Figure 3. Numerical results of streamlines at positive peak disturbances (a) and negative peak disturbances (b). (Q = 0.4 µl/min, Re = 0.048)

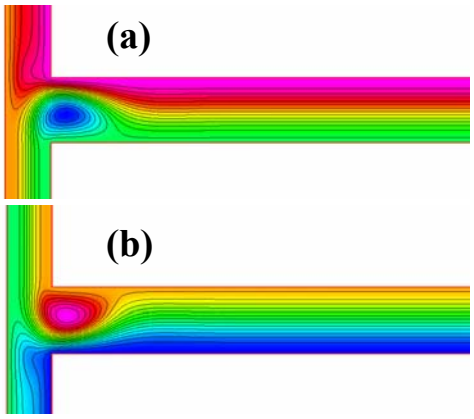

Figure 4. Numerical results of streamlines at positive peak disturbances (a) and negative peak disturbances (b). (Q = 20.0 µl/min, Re = 2.4)

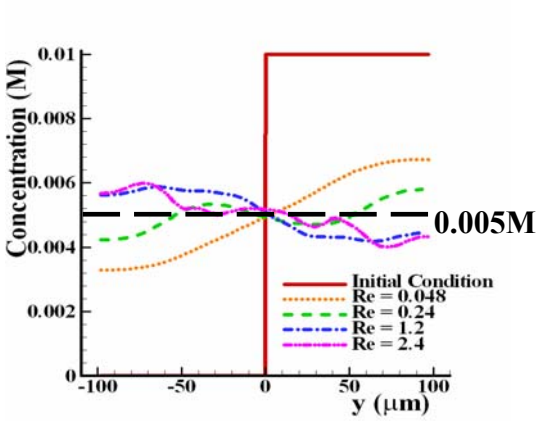

Figure 5. Comparison of profiles of species concentration at x = 3.0 mm and St = 0.56 for different Reynolds numbers.

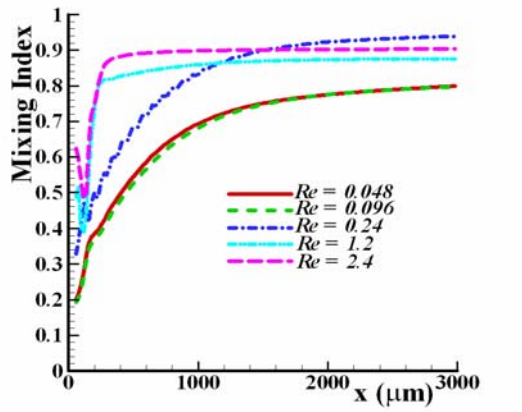

Figure 6. Comparison of distributions of mixing index for different flow rates at fixed St = 0.56.

flow patterns are totally different from that in (a) and (b). This is because the flow velocity in (c) is much higher than that of (a) and (b), and the flow becomes nonlinear. The color of mixture in Fig. 2 (c) turns to green immediately after passing the T-junction. To analyze the flow phenomena in further step, streamlines from numerical simulations are plotted in Fig. 3 for the case shown in Fig. 2 (a), and in Fig. 4 for the case shown in Fig. 2(c). At low Reynolds number (Re = 0.048), it shows in Fig. 3 (a) that there is separation of streamlines at the lower confluence corner, which leads to some of the blue reagent traveling into the inlet for the yellow solution. After half of the period of perturbation, the pulse reached the negative peak value (Fig. 3 (b)), and the blue solution previously flowed into upper inlet was expelled to the horizontal mixing channel. Meanwhile, some of the yellow solution would flow into the lower inlet and repeat the previous process. The pulsing flow stretched and folded the fluids, which significantly increased the contact area and promoted the diffusion effect to achieve good mixing. Very similar results as that shown in Fig.3 were obtained for the case shown in Fig. 2(b) with Re = 0.24, which is not plotted here. Figure 4 shown the streamlines at higher Reynolds number with Re = 2.4. Compared with Fig. 3, the big difference is the generation of vortex near the corner of the T-junction. With the switch of positive and negative peak disturbances, the vortex jumps between the upper and lower corner. The generation of vortex is one of the most efficient methods to achieve chaotic advection and mixing. Consequently, the color of mixture in the main mixing channel becomes almost uniform in the vicinity of T-junction, which means mixing is almost finished in very short distance after confluence.

Figure 5 compares the profiles of species concentration at the outlet of the mixing channel for different flow Reynolds numbers. Red solid line shows the initial condition with a step function. For ideal mixer, the species concentration of the mixture at the outlet should reach 0.005M. It shows in Fig. 5 that the species concentration is more close to the result of an ideal mixer when flow Reynolds number increases and stronger chaotic advection is generated. For

Re ≥ 0.24, the species concentration at the outlet lies in very small range between 0.004M and 0.006M.

To quantitatively evaluate mixing efficiency, mixing index is defined as

$$I = 1.0 - \frac{1}{\bar{c}}\sqrt{\frac{\sum_{i=1}^{N}(c_i - \bar{c})^2\left(\frac{V_i}{\bar{V}}\right)}{N}} \qquad (4)$$

where c_i and V_i are species concentration and mean velocity in the i^{th} cell, respectively, $\bar{c}$ is the mean concentration across channel, and $\bar{V}$ is mean velocity.

Figure 6 compares distributions of mixing index calculated from eqn. (4) for different flow rates at fixed St = 0.56. For very low Reynolds number, Re ≤ 0.096, two cases were studied. The mixing index curves for these two cases are almost same and the maximum mixing index at the outlet is about 0.8. For Re ≥ 0.24, the maximum mixing index is greater than 0.88. It also shows that mixing index increases very fast for x < 1.5mm. After x > 1.5mm, the mixing index does not change too much. From Fig.6, it shows that more than 75% mixing can be finished within a mixing distance of less than 1.5mm from the T-junction for flow Reynolds number less than 0.24. For Reynolds number higher than 0.24, about 90% mixing can be finished in less than 1.5mm. Furthermore, the slopes of mixing index curves increase with increasing Reynolds number, which means the mixing distance is shorter to reach the same mixing index for higher flow rate for fixed St. The reason for faster mixing at high Reynolds number is due to generation of stronger chaotic advection from pressure disturbances.

3 EXPERIMENTAL VALIDATION

Based on the results of numerical simulation, we designed and fabricated the T-mixer. The performance of the mixer was tested by mixing two aqueous solutions with yellow and blue dyes. The flow field was recorded under the microscope by using CCD camera. The image of flow is compared with the numerical results on contour of species concentration. Figure 7 compares the species concentration distribution between numerical results (a, b) and experimental results (c, d) with fixed Re = 0.096 for St = 0.56 and 1.12, respectively. Good agreement in flow patterns between numerical results and experimental results was obtained, which can validate our design of T-form mixer.

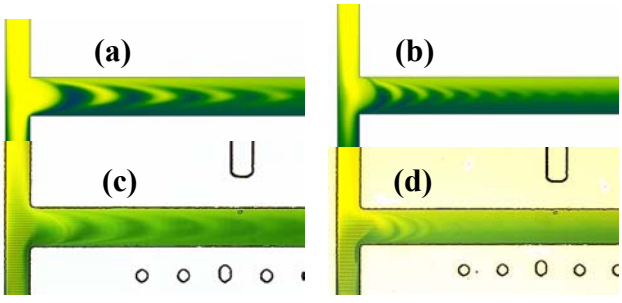

Figure 7. Comparison of species concentration distribution between numerical results (a, b) and experimental results (c, d) with fixed Re = 0.096 for St = 0.56 and 1.12, respectively.

4 ACKNOWLEDGEMENTS

This work was supported by Bioengineering Research Partnership grant EB00127 (to B.M.C.) from the National Institute of Biomedical Imaging and Bioengineering, NIH

REFERENCES

[1] CM. Ho, and YC Tai, "Micro-electro-Mechanical Systems (MEMS) and Fluid Flows", Annu. Rev. Fluid Mech. 30, 1998, pp. 579-612.
[2] D. Erickson and DQ Li, "Integrated Microfluidic Devices", Analytica Chimica Acta, 507, (2004) pp. 11-26.
[3] X. Niu and YK Lee, "Efficient Spatial-Temporal Chaotic Mixing in Microchannels", J. Micromech. Microeng. 13 (2003), pp. 454-462.
[4] V. Hessel, H. Löwe and F. Schönfeld, "Micromixers – A Review on Passive and Active Mixing Principles", Chemical Engineering Science, 60, (2005), pp. 2479-2501.
[5] C. Campbell and B. Grzybowski, "Microfluidic Mixers: from Microfabricated to Self-Assembling Devices", Phil. Trans. R. Soc. Lond. A. 362, (2004), pp.1069-1086.
[6] NT guyen and ZG Wu, "Micromixers – a Review", J. Micromech. Microeng. 15 (2005), pp. R1-R16.
[7] I. Glasgo and N. Aubry, "Enhancement of Microfluidic Mixing Using Pulsing", Lab Chip, 3, (2003), pp. 114-120.
[8] I. Glasgow, S. Lieber and N. Aubry, "Parameters Influencing Pulsed Flow Mixing in Microchannels", Analytical Chemistry, 76, (2004), pp. 4825-4832.